PHARMACOLOGY

Molecular overlap in the regulation of SK channels by small molecules and phosphoinositides

Miao Zhang,[1,2]* Xuan-Yu Meng,[1†] Ji-fang Zhang,[3,4] Meng Cui,[1] Diomedes E. Logothetis[1]*

Phosphatidylinositol 4,5-bisphosphate (PIP_2) directly interacts with the small-conductance Ca^{2+}-activated K^+ 2-a (SK2-a) channel/calmodulin complex, serving as a critical element in the regulation of channel activity. We report that changes of protein conformation in close proximity to the PIP_2 binding site induced by a small-molecule SK channel modulator, NS309, can effectively enhance the interaction between the protein and PIP_2 to potentiate channel activity. This novel modulation of PIP_2 sensitivity by small-molecule drugs is likely not to be limited in its application to SK channels, representing an intriguing strategy to develop drugs controlling the activity of the large number of PIP_2-dependent proteins.

INTRODUCTION

The small- and intermediate-conductance Ca^{2+}-activated K^+ (SK/IK) channels play important roles in the regulation of membrane excitability by Ca^{2+} (1–4). Activation of SK channels by small molecules in the nucleus accumbens region of the brain could help treat alcohol addiction (5). Administration of positive SK channel modulators is beneficial in animal models of neurodegenerative diseases, such as ataxia (6). Tremendous effort has been devoted to developing small molecules targeting SK/IK channels, including the most potent positive modulator NS309 (7–13), that enhance SK/IK channel activity through allosteric modulation. Some of these compounds, such as chlorzoxazone and riluzole (Rilutek), have been used in multiple clinical trials for neurological disorders, such as alcoholism and cerebellar ataxia (http://clinicaltrials.gov/).

SK/IK channels are not voltage-dependent but are exclusively activated by Ca^{2+}-bound calmodulin (CaM) tethered to the CaM-binding domain (CaMBD) located at the C terminus of the channel (14, 15). Binding of Ca^{2+} to CaM causes significant changes in the conformations for both CaM and CaMBD, leading to formation of a complex between CaM and CaMBD (16–18). CaM associated with CaMBD is responsible for Ca^{2+} sensing, whereas the transmembrane helices are the place where mechanical gating occurs. Between the S6 (the last transmembrane helix) and the CaMBD lies the channel fragment R396-M412, the conformation of which is critical for the coupling between Ca^{2+} sensing by CaM and channel opening (19). Pharmacological intervention with NS309 stabilizes this channel fragment and facilitates channel opening. However, it has remained unknown which physiological factor is responsible for the coupling. Here, we show that phosphatidylinositol 4,5-bisphosphate (PIP_2) is the physiological

regulator that modulates the coupling to channel opening and that NS309 enhances the PIP_2 interactions with the CaM/SK2 complex to exert its effect.

RESULTS

The influence of NS309 on the intrinsically disordered protein fragment conformation of the SK2-a channel

The SK2 channel opens in response to elevated intracellular Ca^{2+} levels. Ca^{2+} binds to CaM associated with CaMBD at the channel C terminus and induces conformational changes. The Ca^{2+}-induced conformational changes are transmitted to the transmembrane domains through an SK2 channel fragment. Part of this SK2 channel fragment (E399-K402) forms a "cuff" that interacts with the CaM linker region between the N- and C-lobes. The rest (E404-M412) is highly flexible, and as a result, its conformation could not be determined by x-ray crystallography [Protein Data Bank (PDB): 4J9Y] in the absence of NS309 (Fig. 1A). This highly flexible fragment exhibited the characteristics of an intrinsically disordered protein fragment (IDF) (19). For instance, the side chain of E404 is highly flexible and cannot be determined beyond the β carbon. Along the direction of the β carbon, the side chain was modeled with PyMOL. The putative E404 side chain (δ carbon) is 5.5 Å away from R471 (ζ carbon), suggesting a possible salt bridge between the two residues. We examined this possibility using molecular dynamics (MD) simulations. Indeed, during a 20-ns simulation, the distance between E404 and R471 mostly stayed below 5 Å, indicating a stable salt bridge (fig. S1A and Fig. 1A). In the cocrystal structure with NS309 (PDB: 4J9Z), NS309 stabilizes the IDF, and the electron density showed a well-structured IDF (Fig. 1C). NS309 formed a hydrogen bond with K75 of CaM, which, in turn, promoted the salt bridge E404-K75. Consistently, MD simulations with NS309 showed that E404 no longer formed a salt bridge with R471 (as it did in Fig. 1B in the absence of NS309), but rather it formed a salt bridge with K75 (3.8 Å) (fig. S1B and Fig. 1D). NS309 left-shifted the Ca^{2+} median effective concentration (EC_{50}) by about sixfold from 0.32 ± 0.3 μM ($n = 8$) to 0.052 ± 0.03 μM ($n = 5$; $P < 0.01$) (Fig. 1, E and F), consistent with our previous work (19). The single mutant E404A/C/D or K75C/R failed to be activated by Ca^{2+}, whereas the double mutant E404D/K75R rescued activation by Ca^{2+} and

[1]Department of Physiology and Biophysics, Virginia Commonwealth University School of Medicine, 1101 East Marshall Street, Richmond, VA 23298, USA. [2]Department of Biomedical and Pharmaceutical Sciences, Chapman University School of Pharmacy, 9401 Jeronimo Road, Irvine, CA 92618, USA. [3]Department of Molecular Physiology and Biophysics, Thomas Jefferson University, 1020 Locust Street, Philadelphia, PA 19107, USA. [4]Farber Institute for Neurosciences and Graduate Program in Neuroscience, Thomas Jefferson University, 1020 Locust Street, Philadelphia, PA 19107, USA.
*Corresponding author. E-mail: zhang@chapman.edu (M.Z.); delogothetis@vcu.edu (D.E.L.)
†Present address: School for Radiological and Interdisciplinary Sciences, Collaborative Innovation Center of Radiation Medicine of Jiangsu Higher Education Institutions, and Jiangsu Provincial Key Laboratory of Radiation Medicine and Protection, Soochow University, Suzhou 215123, China.
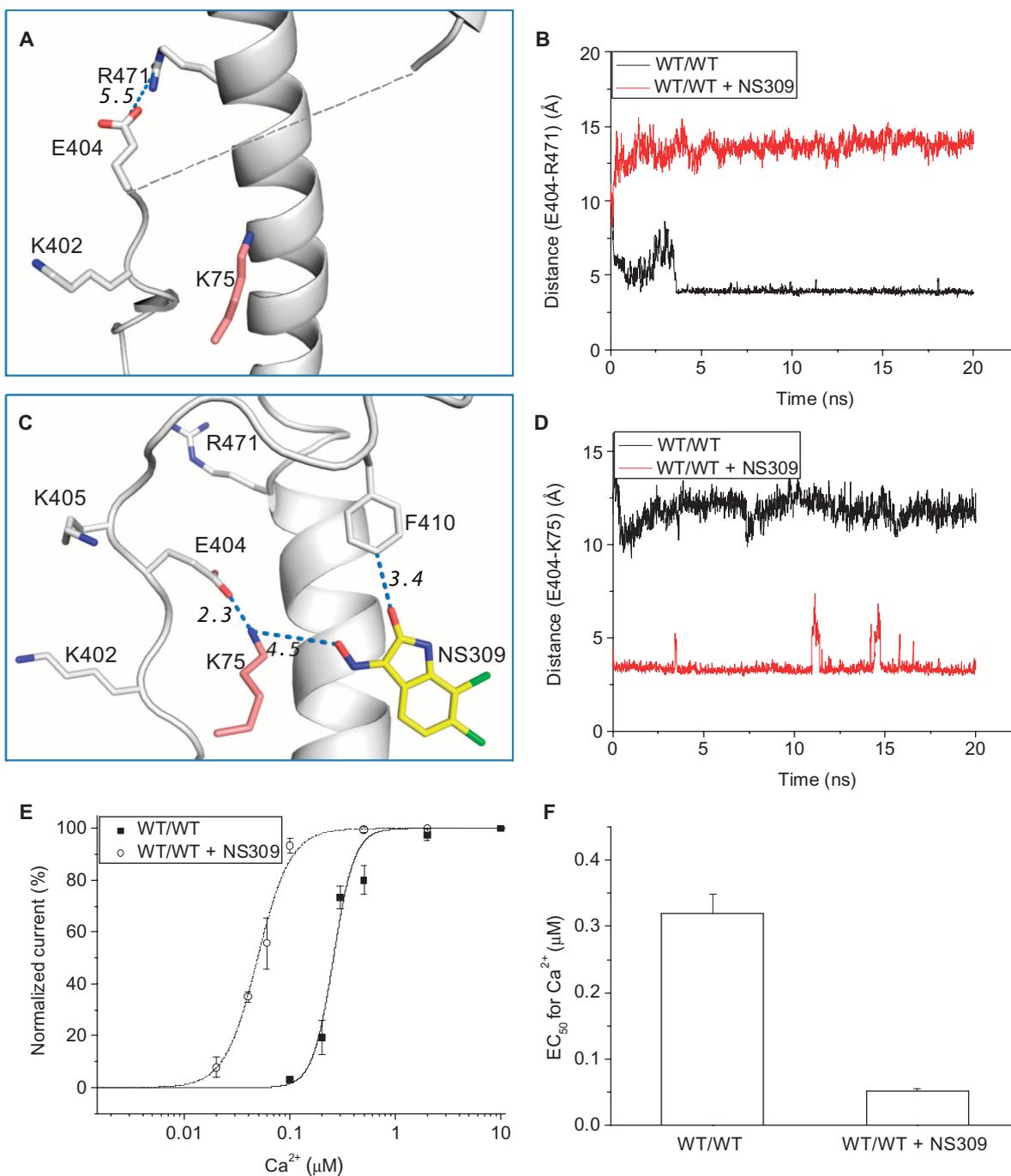
Fig. 1. Stabilization of IDF of SK2-a channel by NS309. (**A**) The IDF (dashed line) is highly flexible in the absence of NS309, and its structure could not be determined by x-ray crystallography. (**B**) E404-R471 distance from MD simulation in the absence (black) and presence (red) of NS309. (**C**) The IDF becomes well structured in the presence of NS309. NS309 forms contacts with F410. In addition, the E404-K75 salt bridge is promoted through a hydrogen bond between NS309 and K75. (**D**) The E404-K75 distance from MD simulations in the absence (black) and presence (red) of NS309. (**E**) Dose-response curves of channel reactivation by Ca^{2+} in the absence (solid line, filled symbols) and presence (dashed line, open symbols) of 3 μM NS309 of the wild-type (WT)/WT (SK2-a/CaM) channel. (**F**) NS309 increases the apparent affinity for Ca^{2+} of SK2-a channels.

NS309, similarly left-shifting the Ca^{2+} EC$_{50}$ by about sevenfold (*19*). It was postulated that the salt bridge formation by these two residues must be important for channel opening. However, interactions between a fluorophore-labeled CaM and the CaMBD of SK2-a showed no evidence for changes in Ca^{2+} binding by either NS309 or mutants that produced clear changes in Ca^{2+} responses (*19*). These results suggested that NS309 and the IDF mutants acted downstream of Ca^{2+} binding, closer to the channel-gating machinery.

PIP$_2$ in regulation of SK2-a channel

R396 is the last residue of the S6 transmembrane domain, which makes the CaM linker, the cuff (E399-K402), and IDF (E404-M412) accessible to the inner leaflet of the plasma membrane. This region is rich in positively charged residues. In the past couple of decades, it has been established that plasma membrane phosphoinositides, mainly PIP$_2$, can regulate the activities of many different types of ion channels (20–22). The PIP$_2$ binding site consists of positively charged amino acid residues clustered close to the bottom of the pore-forming S6 segments and the immediate C-linker region connecting the S6 transmembrane domain to the cytosolic domain of each channel protein (23–26). As Fig. 2A shows, with combined approaches of MD simulation and site-directed mutagenesis, we recently identified a putative binding site for PIP$_2$ in SK2-a channels, which involves K402 and K405 from the channel, in addition to K77 and R74 (not shown) of the CaM linker region (27). This region is distant from the Ca^{2+}-binding sites (EF hands) of CaM. Because residues in this region were shown not to interfere with Ca^{2+} binding (19), PIP$_2$ could serve as the physiological regulator responsible for the coupling between the Ca^{2+} binding of CaM and the mechanical opening of the channel pore. In MD simulations, PIP$_2$ prominently influenced the conformation of E404. PIP$_2$ disrupted the E404-K471 salt bridge (fig. S2A), whereas it promoted the E404-K75 salt bridge (Fig. 2A and fig. S2B), similar to the effect of NS309.

Proximity of NS309 binding pocket and the putative PIP$_2$ binding site

We used MD simulations to examine interactions between PIP$_2$ and its binding site in the absence (Fig. 2, A and B) and presence (Fig. 2, C and D)

of NS309. Without NS309, the P4 phosphate of PIP$_2$ primarily interacts with K402 and K405, whereas P5 forms salt bridges with K77 and K402 (Fig. 2B). In the presence of NS309, a strengthened salt bridge between the P5 of PIP$_2$ and K405 of the IDF was observed (Fig. 2D). The histogram of the P5-K405 distance from the MD simulations confirmed the clear difference between the presence and absence of NS309 (fig. S3A). In the absence of NS309, the P5-K405 distance broadly distributes, with the major peak larger than 7 Å. With NS309, the P5-K405 distance peaks at 3.8 Å, clearly showing a high probability for salt bridge formation (fig. S3A). The distances between P5-K402, P4-K405, and P4-K402 are not essentially affected by NS309 (fig. S3, B to D, and Fig. 2, A and B versus C and D).

Our previous work (19, 27) has suggested that both NS309 and PIP$_2$ are involved in the coupling between Ca^{2+} sensing by CaM and channel gating. Together with the proximity of their binding sites (Fig. 2C), this overlap in their function motivated us to test whether NS309 cooperates with PIP$_2$ in modulation of SK2-a channel activity. It is clear that PIP$_2$ alone is effective in this coupling to channel opening because the channel can open in the absence of NS309. However, it is unknown whether NS309 can replace PIP$_2$ and open the channel in the absence of PIP$_2$. SK channel currents were recorded using inside-out patches, as previously described (18, 19, 28). Upon application of poly-lysine (poly-K, 900 μg/ml), shown to sequester endogenous PIP$_2$ (29, 30), the current was almost completely inhibited (Fig. 3A). Saturating concentrations of Ca^{2+} (2 μM) and NS309 (3 μM) were applied to the cytoplasmic side of the patch but failed to induce any current (Fig. 3A), suggesting that PIP$_2$ could not be replaced by NS309 in coupling Ca^{2+} binding to SK2-a channel opening.

Because NS309 could not replace PIP$_2$, its potentiation of channel activity could be working through an increase in PIP$_2$ sensitivity. To
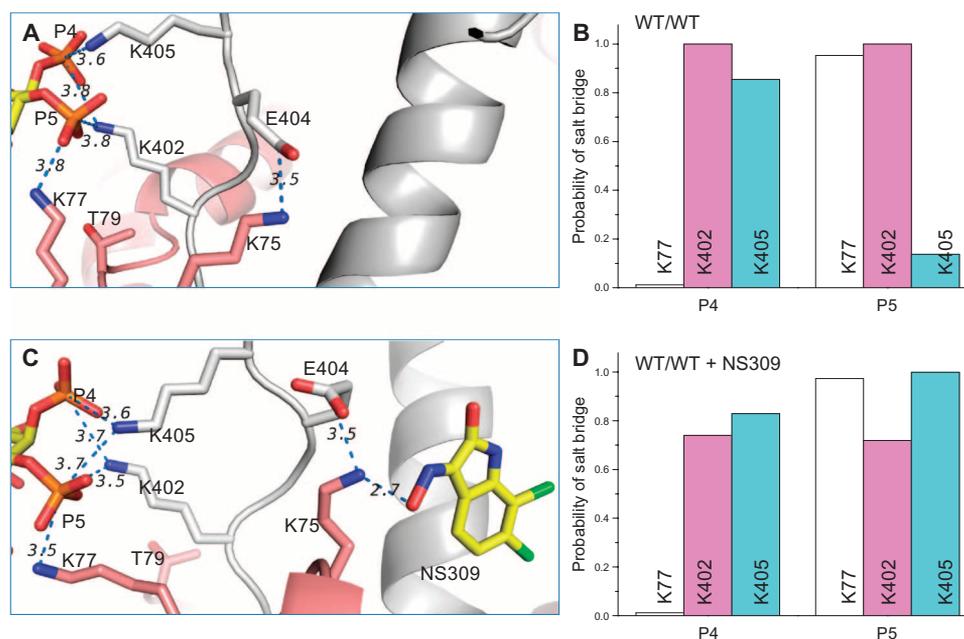
Fig. 2. The effect of NS309 on PIP$_2$ interactions with SK2-a channel. (**A**) A representative snapshot from MD simulations of PIP$_2$ (P4 and P5 in orange and oxygens in red) binding to CaM (salmon) and SK2-a channel (gray) in the absence of NS309. (**B**) Summarized probability of forming salt bridges between PIP$_2$ head and positively charged residues in the absence of NS309. (**C**) A representative snapshot from MD simulations of PIP$_2$ (P4 and P5 in orange and oxygens in red) binding to CaM and SK2-a channel (gray) in the presence of NS309 (yellow). Salt bridges are shown as blue dashed lines with distances in angstrom. (**D**) Summarized probability of forming salt bridges between the PIP$_2$ head and positively charged residues in the presence of NS309.
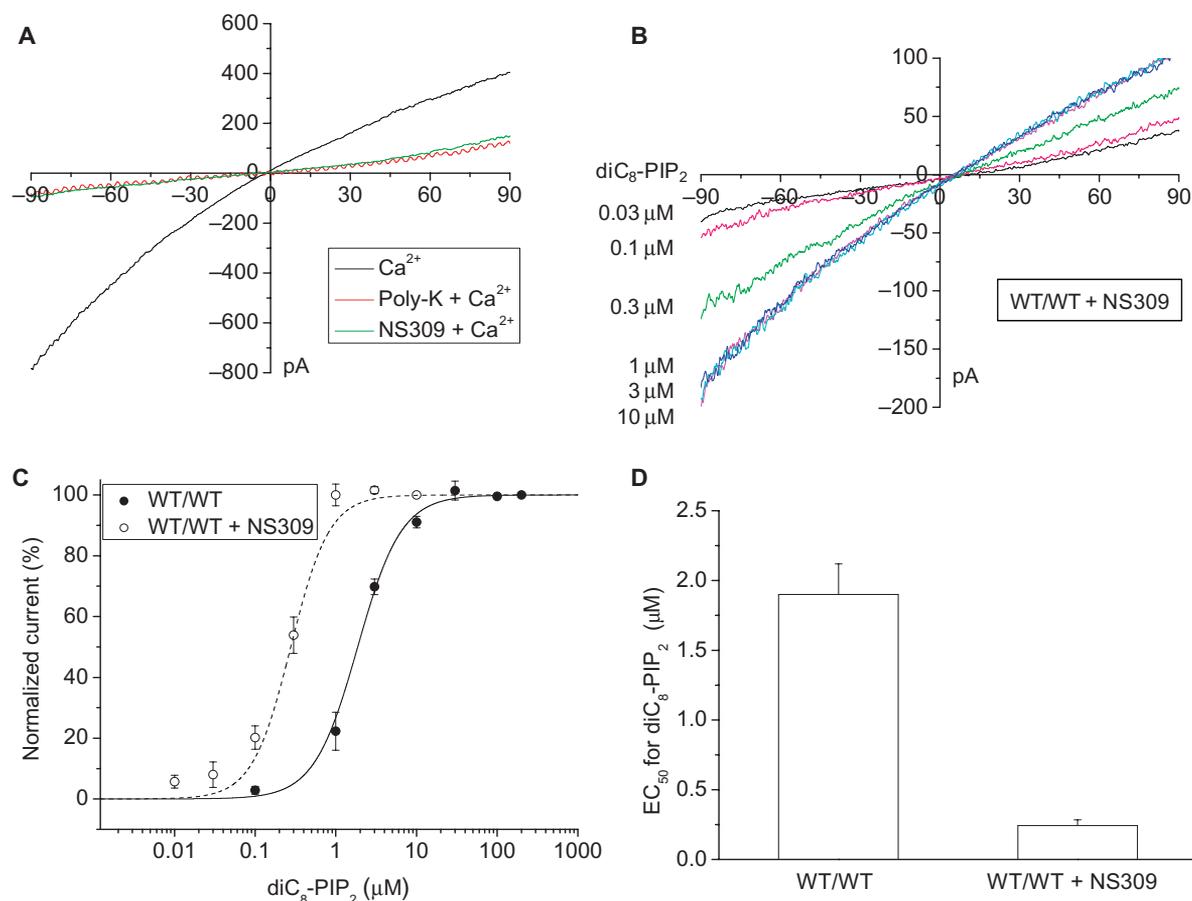
Fig. 3. The effect of NS309 on PIP$_2$ sensitivity of the SK2-a channel. (**A**) Raw current traces before (black) and after (red) application of poly-K in the presence of 2 μM Ca^{2+}. After depletion of endogenous PIP$_2$, 2 μM Ca^{2+} and 3 μM NS309 (green) could not induce any measurable current increase. (**B**) Dose-dependent channel reactivation by exogenous diC$_8$-PIP$_2$ at the indicated concentrations, in the presence of 3 μM NS309, after depletion of the endogenous PIP$_2$ by poly-K. (**C**) Dose-response curves of channel reactivation by exogenous diC$_8$-PIP$_2$ in the absence (solid line) and presence (dashed line) of 3 μM NS309 on WT/WT (SK2-a/CaM) channel. (**D**) NS309 increases the apparent affinity for diC$_8$-PIP$_2$ of SK2-a channels.

evaluate the effect of NS309 on PIP$_2$ sensitivity, a water-soluble, synthetic PIP$_2$ derivative, diC$_8$-PIP$_2$, together with NS309 (3 μM) and Ca^{2+} (2 μM), was gradually applied to the bath solution once the sequestration of the endogenous PIP$_2$ by poly-K was achieved (Fig. 3B). Application of diC$_8$-PIP$_2$ restored the SK current in a dose-dependent manner (Fig. 3, B and C), with the EC$_{50}$ for diC$_8$-PIP$_2$ at 1.9 ± 0.22 μM in the absence of NS309 (n = 6; Fig. 3, C and D). In the presence of NS309 (3 μM), the dose-response curve of diC$_8$-PIP$_2$ was left-shifted (Fig. 3C), with the EC$_{50}$ for diC$_8$-PIP$_2$ at 0.24 ± 0.04 μM (n = 4; P < 0.01; Fig. 3, C and D).

SK2-a channels have been shown to be regulated by phosphorylation or dephosphorylation (31–33). Phosphorylation of CaM at T79 by casein kinase II reduces the Ca^{2+} sensitivity of the SK2-a/CaM complex for channel activation (32). CaM T79 is located in the vicinity of the PIP$_2$ binding site (Fig. 2A). Mimicked by T79D, its phosphorylation can significantly reduce the apparent affinity of PIP$_2$ for its binding site and therefore exert its inhibitory effect on channel activity (27). In response to neurotransmitters such as noradrenaline and acetylcholine, the SK channel/CaM complex undergoes phosphorylation at T79, which results in inhibition of SK channel activity (33–35). The question arises whether this phosphorylated form of the SK2-a

channel/CaM complex is sensitive to pharmacological intervention using small molecules such as NS309. We set out to clarify this question with the phosphomimetic T79D mutant channel. NS309 (3 μM) significantly reduced the EC$_{50}$ for PIP$_2$ on the T79D mutant channel (1.89 ± 0.36 μM; n = 5; P = 0.005) compared with 22.1 ± 2.22 μM (n = 4) in the absence of NS309 (fig. S4, A and B). Under physiological conditions, the CaM molecules complexed with the SK channel undergo dynamic changes in their phosphorylation status (31, 32). The capability of NS309 to modulate both the phosphorylated and dephosphorylated channel complexes is of practical interest, considering the application of positive SK channel modulators in vivo as potential therapeutic agents.

The phosphomimetic T79D mutation causes a substantial conformational change at the PIP$_2$ binding site (fig. S5A) compared with the WT/WT channel/CaM complex (Fig. 2A). The P4-K402 and P5-K77 interactions are weakened, whereas the P5-K405 interaction is strengthened (Fig. 2B versus fig. S5B). T79D is neighbored by K402 and K77. The negative charge at T79D inevitably interferes with the P4-K402 and P5-K77 interactions, which are only partially compensated by the strengthened P5-K405 interaction (fig. S5B). Overall, the PIP$_2$ interaction is weakened by the negative charge of T79D mutation. The binding of NS309 partially

restores the PIP$_2$ interaction (fig. S5C). It causes a significant rearrangement of the PIP$_2$ binding site (fig. S5D versus fig. S5B). The P5-K402 interaction is weakened, whereas both the P4-K77 and the P4-K402 interactions are enhanced, resulting in a net gain in interaction with PIP$_2$. The enhancement of the P4-K77 (fig. S6A) and the P4-K402 (fig. S6B) interactions is reflected by the shortening of their distance from each other in the MD simulations. The weakening of the P5-K402 interaction is reflected by an increase in distance (fig. S6C). The P5-K405 distance is not affected by NS309 (fig. S6D).

Role of PIP$_2$ in the effect of NS309

Because NS309 and Ca^{2+} cannot open the channel in the absence of PIP$_2$ (Fig. 3A), we turned to a different strategy to examine the role of PIP$_2$ in the effect of NS309. We identified several mutations that interfere with the regulation of the channel by PIP$_2$, such as the SK2-a K402, K405, and the phosphomimetic CaM T79D mutations (Fig. 4A). The PIP$_2$ sensitivity was determined through scavenging of endogenous PIP$_2$ with poly-K and reintroducing it by subsequent application of diC$_8$-PIP$_2$ in the bath solution, as in Fig. 3 (B and C). Compared with the EC$_{50}$ for diC$_8$-PIP$_2$ at 1.9 ± 0.22 μM for WT/WT channel (n = 6), the mutations of K402N, K405N, and T79D significantly reduced the

apparent affinity of PIP$_2$, with EC$_{50}$ at 14.2 ± 1.93 μM (n = 4; P < 0.001), 15.2 ± 2.14 μM (n = 4; P < 0.001), and 22.1 ± 2.22 μM (n = 4; P < 0.001), respectively (Fig. 4A). We continued by testing the effect of NS309 on these mutant channels (Fig. 4B). The EC$_{50}$ values for NS309 in these mutant channels were significantly increased compared to those in the WT/WT channel (0.24 ± 0.031 μM; n = 6). The EC$_{50}$ values of NS309 for the K402N, K405N, and T79D mutants were 0.49 ± 0.047 μM (n = 5; P < 0.001), 0.46 ± 0.067 μM (n = 5; P = 0.002), and 0.67 ± 0.043 μM (n = 4; P < 0.001), respectively. There is a clear correlation (R = 0.981) between the sensitivity of the mutant channels toward NS309 and PIP$_2$ (Fig. 4C). Figure 4D shows a simplified scheme for SK2-a channel activation, with Ca^{2+} binding to CaM as the first step and the mechanical coupling to channel opening as the second step. Both PIP$_2$ and NS309 act on the second step. Because PIP$_2$ is the necessary factor for the NS309 effect (Fig. 3A), a reasonable interpretation would be that NS309 facilitates regulation of channel opening by PIP$_2$ (Fig. 3D) and potentiates channel activity. Although NS309 primarily strengthens the K405-P5 interaction as shown in the MD simulation (Fig. 2D), K405N did not abolish the potentiation of SK2-a channels by NS309. Rather, K405N mutation reduces the potency of NS309 in a manner correlated to its weakening
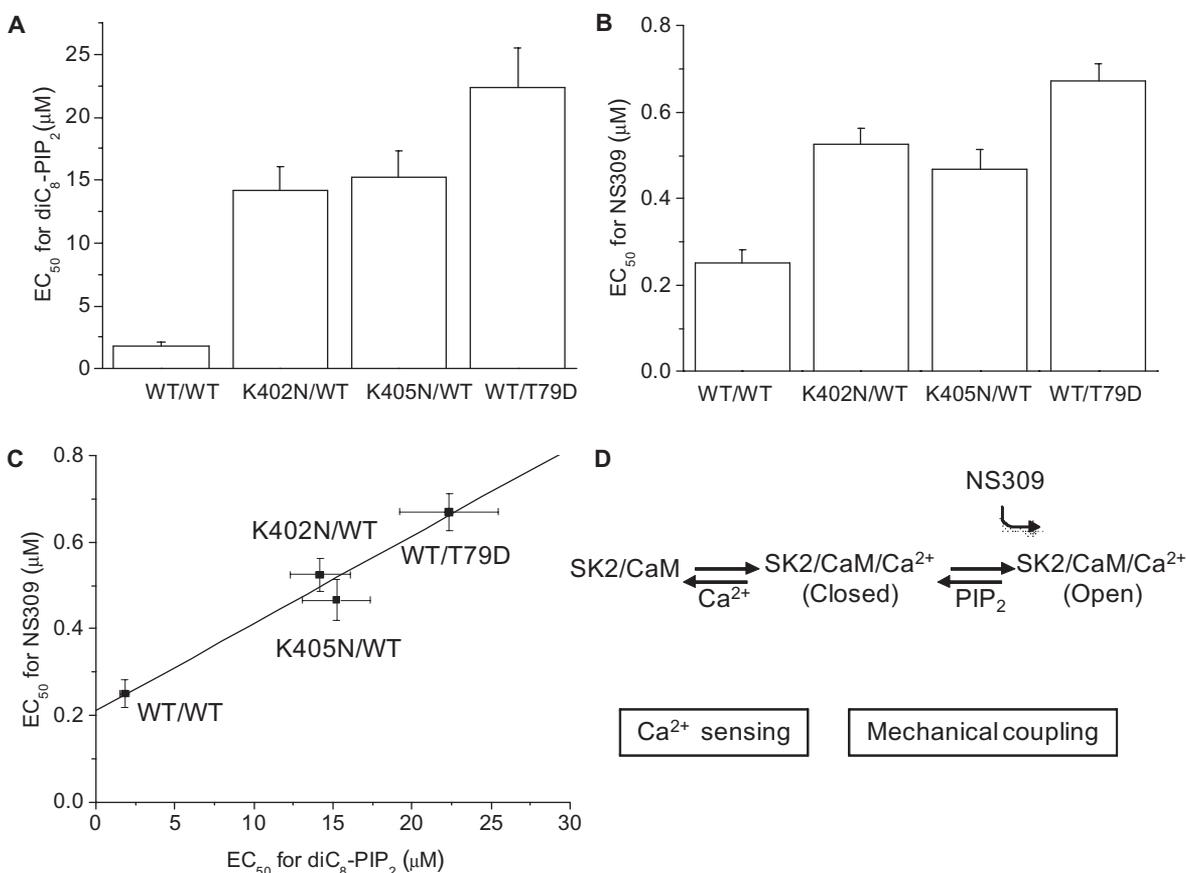

Fig. 4. The role of PIP$_2$ in the effect of NS309. (**A**) Mutant channels that show decreased apparent affinity for diC$_8$-PIP$_2$. (**B**) The same group of mutations also decreases potency of NS309. (**C**) A clear correlation between PIP$_2$ sensitivity and NS309 potency on the mutant channels (R = 0.981). (**D**) A simplified scheme for SK2-a channel activation, with Ca^{2+} binding to CaM as the first step and PIP$_2$-mediated coupling to channel opening as the second step. PIP$_2$ does not activate the channel in the absence of Ca^{2+}. NS309 potentiates channel activity through an enhancement of function by strengthening channel-PIP$_2$ interactions.

Zhang et al. Sci. Adv. 2015;1:e1500008   10 July 2015

5 of 8

of channel-PIP$_2$ interactions (Fig. 4C), suggesting the central role of channel-PIP$_2$ interactions in the mechanism of action of NS309.

DISCUSSION

NS309 enhances the Ca^{2+} sensitivity of SK channel and thus was previously speculated to change the Ca^{2+} binding to CaM associated with SK channels. Subsequently, we suggested that NS309 does not influence the Ca^{2+} binding to CaM and the Ca^{2+}-induced conformational change of the CaM/CaMBD complex (19). Rather than Ca^{2+}, here we show that NS309 allosterically enhances the interactions of PIP$_2$ with the CaM/SK2 complex as its mechanism of action.

PIP$_2$ is a necessary cofactor for the function of many ion channels, regulating channel activity through direct interactions (20, 21). Considering this crucial role of PIP$_2$-channel interactions in ion channel function, changes in these interactions would inevitably influence channel activity. Here, we have demonstrated that NS309 enhances the PIP$_2$ sensitivity of both the WT/WT channel/CaM complex (Fig. 3) and a phosphomimetic CaM mutant/channel complex (fig. S4) and thus positively modulates the SK channel activity. A recent study has shown that PIP$_2$ exists in the plasma membrane at nanoscale regions (36) and may reach relatively high local concentrations. Neurotransmitters induce phosphorylation of CaM associated with SK channels, which results in reduced PIP$_2$ sensitivity of SK channels (27). Meanwhile, the neurotransmitters such as acetylcholine may also induce hydrolysis and thus reduce PIP$_2$ levels (27). These synergistic effects can potently inhibit SK channel activity. Under such circumstances, the ability of compounds to positively modulate the phosphorylated form (mimicked by T79D) of SK channels is essential for their drug effects. To date, NS309 represents a unique example of pharmacological modulation of ion channels by small molecules through manipulation of channel-PIP$_2$ interactions. However, it is unlikely that NS309 is the only compound that modulates channel activity through this mechanism. It will not be surprising if additional drugs targeting ion channels are found to act on modulating channel-PIP$_2$ interactions. The present work ought to motivate the development of new compounds targeting ion channels through allosteric weakening or enhancement of channel-PIP$_2$ interactions. Recent work from our group has shown that, in addition to ion channels, other transmembrane proteins such as tyrosine kinase receptors may also be regulated by PIP$_2$ (37). Most recently, the psychostimulant amphetamine has been found to alter the PIP$_2$ interaction of human dopamine transporter and trigger dopamine efflux (38). Therefore, the strategy for developing drugs that modulate protein-PIP$_2$ interactions is likely not to be limited to ion channels.

MATERIALS AND METHODS

Molecular biology and channel expression

Details can be found in our previous papers (18, 19, 28). Briefly, rat SK2-a channels (accession no. NM_019314), along with CaM (accession no. NM_012518), were each subcloned into the pCDNA3.1(+) expression vector (Invitrogen). Mutations were introduced into SK2-a or CaM using the QuikChange XL Site-Directed Mutagenesis Kit (Stratagene-Agilent) and subsequently confirmed by DNA sequencing. Along with WT CaM or mutant CaM and green fluorescent protein,

WT or mutant channels were expressed in TsA201 cells cultured in Dulbecco's modified Eagle's medium supplemented with 10% fetal bovine serum and penicillin/streptomycin. The calcium phosphate method was used for transfection of SK2-a complementary DNA (WT or mutants), together with WT CaM or mutant CaM and green fluorescent protein at a ratio of 5:2.5:1 (weight). SK channel modulator NS309 was from Tocris. DiC$_8$-PIP$_2$ was from Avanti Polar Lipids. Poly-K was purchased from Sigma-Aldrich.

Electrophysiology

Channel activities were recorded with the inside-out patch clamp configuration 1 to 2 days after transfection, with a MultiClamp 700B or an Axon 200B amplifier (Molecular Devices) at room temperature. pCLAMP 10.2 (Molecular Devices) was used for data acquisition and analysis. The resistance of the patch electrodes ranged from 3 to 6 megohms. The pipette solution contained 140 mM KCl, 10 mM Hepes, and 1 mM MgSO$_4$ (pH 7.4). The bath solution contained 140 mM KCl and 10 mM Hepes (pH 7.2). EGTA (1 mM) and HEDTA (hydroxyethyl ethylenediaminetriacetic acid) (1 mM) were mixed with Ca^{2+} to obtain the indicated free Ca^{2+}, calculated using the software by C. Patton of Stanford University (www.stanford.edu/~cpatton/maxc.html). The Ca^{2+} concentrations were verified using Fluo-4 and standard Ca^{2+} buffers (Molecular Probes). Currents were recorded by repetitive 1-s voltage ramps from −100 to +100 mV from a holding potential of 0 mV. For dose-response curves of NS309 in the presence of Ca^{2+} (0.2 μM), the current amplitudes at −90 mV in response to various NS309 concentrations were normalized to that obtained at a maximal NS309 concentration. The dose-response curves for diC$_8$-PIP$_2$ were obtained at various diC$_8$-PIP$_2$ concentrations in the presence of 2 μM Ca^{2+}, with or without NS309 (3 μM) after successful depletion of the native PIP$_2$ by poly-K (900 μg/ml) and subsequent washout of the poly-K. EC$_{50}$s for NS309 or diC$_8$-PIP$_2$ were determined by fitting the data points to the Hill equation $[Y = 100/(1 + (X/EC_{50})^{-\text{Hill}})]$.

Molecular docking

The molecular docking program AutoDock 4 (39) was used for the docking of PIP$_2$ into the structure of the CaM/CaMBD complex (4J9Z) (19). The partial charges for PIP$_2$ were obtained from ab initio quantum chemistry at the Hartree-Fock (HF)/6-31+G* level using the CHELPG (charges from electrostatic potentials using a grid-based method) charge–fitting scheme (40) of Gaussian 98 program (41) as described previously (42). Because the size of the PIP$_2$ molecule is too large for flexible docking studies, we replaced it with an analog (diC$_1$), which replaces the two long tails of PIP$_2$ by two methyl groups. Grid potential maps were generated for the CaM/CaMBD complex using CHNOP (that is, carbon, hydrogen, nitrogen, oxygen, and phosphorus) elements sampled on a uniform grid containing 60 × 60 × 58 points, 0.375 Å apart. The center of the grid box was set to a critical PIP$_2$-sensitive residue, K77. The Lamarckian genetic algorithm was selected to identify the binding conformations of the ligands. The side chains for residues R74, K77, K402, and K405 were set to be flexible. One hundred docking simulations were performed, and the final docked diC$_1$-PIP$_2$ configurations were selected on the basis of docked binding energies and relative orientation of the diC$_1$-PIP$_2$ to the CaM/CaMBD complex.

MD simulations

Complexes of CaM/CaMBD or CaM(T79D)/CaMBD and diC$_1$-PIP$_2$ in the presence and absence of NS309 were immersed in 0.15 M KCl

virtual solution. The OPLS (optimized potentials for liquid simulations) force field was used for CaM/CaMBD and diC$_1$-PIP$_2$, and the simple point charge (SPC) model for water molecules. All MD simulations were carried out using Desmond 3.1 (*43*). After being relaxed by the Desmond standard NPT (constant number of atoms, pressure, and temperature) relaxation protocol, complexes were subjected to 20-ns MD simulations without any restraint at the constant temperature of 298 K. The distance distribution histograms between different amino acid residues or between amino acid residues and the PIP$_2$ head were constructed and fit to Gaussian distribution functions to obtain the mean distances. A total of 2001 models were generated during the MD simulation. Structure graphics were created using PyMOL (Schrödinger, LLC).

Statistical analysis

All data are presented as means ± SEM. The Student *t* test was used for data comparisons.

SUPPLEMENTARY MATERIALS

Supplementary material for this article is available at http://advances.sciencemag.org/cgi/content/full/1/6/e1500008/DC1

Fig. S1. The influence of NS309 on the conformation of IDF.
Fig. S2. The influence of PIP$_2$ on the conformation of the IDF.
Fig. S3. The PIP$_2$-channel interaction is affected by NS309.
Fig. S4. The effectiveness of NS309 on the phosphomimetic T79D CaM mutant.
Fig. S5. The proximity of NS309 and CaM T79D mutation to the PIP$_2$ binding site.
Fig. S6. The PIP$_2$-channel interaction is affected by NS309 in the context of T79D mutant.

REFERENCES AND NOTES

1. M. Stocker, Ca^{2+}-activated K$^+$ channels: Molecular determinants and function of the SK family. *Nat. Rev. Neurosci.* **5**, 758–770 (2004).
2. J. P. Adelman, J. Maylie, P. Sah, Small-conductance Ca^{2+}-activated K$^+$ channels: Form and function. *Annu. Rev. Physiol.* **74**, 245–269 (2012).
3. E. S. L. Faber, P. Sah, Functions of SK channels in central neurons. *Clin. Exp. Pharmacol. Physiol.* **34**, 1077–1083 (2007).
4. H. Wulff, A. Kolski-Andreaco, A. Sankaranarayanan, J. M. Sabatier, V. Shakkottai, Modulators of small- and intermediate-conductance potassium channels and their therapeutic indications. *Curr. Med. Chem.* **14**, 1437–1457 (2007).
5. F. W. Hopf, M. S. Bowers, S. J. Chang, B. T. Chen, M. Martin, T. Seif, S. L. Cho, K. Tye, A. Bonci, Reduced nucleus accumbens SK channel activity enhances alcohol seeking during abstinence. *Neuron* **65**, 682–694 (2010).
6. A. W. Kasumu, C. Hougaard, F. Rode, T. A. Jacobsen, J. M. Sabatier, B. L. Eriksen, D. Strøbæk, X. Liang, P. Egorova, D. Vorontsova, P. Christophersen, L. C. Rønn, I. Bezprozvanny, Selective positive modulator of calcium-activated potassium channels exerts beneficial effects in a mouse model of spinocerebellar ataxia type 2. *Chem. Biol.* **19**, 1340–1353 (2012).
7. P. Pedarzani, M. Stocker, Molecular and cellular basis of small- and intermediate-conductance, calcium-activated potassium channel function in the brain. *Cell. Mol. Life Sci.* **65**, 3196–3217 (2008).
8. A. Girault, J. P. Haelters, M. Potier-Cartereau, A. Chantôme, P. A. Jaffrés, P. Bougnoux, J. Joulin, C. Vandier, Targeting SKCa channels in cancer: Potential new therapeutic approaches. *Curr. Med. Chem.* **19**, 697–713 (2012).
9. T. Blank, I. Nijholt, M.-J. Kye, J. Spiess, Small conductance Ca2+-activated K+ channels as targets of CNS drug development. *Curr. Drug Targets CNS Neurol. Disord.* **3**, 161–167 (2004).
10. J. Liégeois, F. Mercier, A. Graulich, F. Graulich-Lorge, J. Scuvée-Moreau, V. Seutin, Modulation of small conductance calcium-activated potassium (SK) channels: A new challenge in medicinal chemistry. *Curr. Med. Chem.* **10**, 625–647 (2003).
11. H. Wulff, B. S. Zhorov, K$^+$ channel modulators for the treatment of neurological disorders and autoimmune diseases. *Chem. Rev.* **108**, 1744–1773 (2008).
12. H. Wulff, M. J. Miller, W. Hänsel, S. Grissmer, M. D. Cahalan, K. G. Chandy, Design of a potent and selective inhibitor of the intermediate-conductance Ca^{2+}-activated K$^+$ channel, *IKCa1*: A potential immunosuppressant. *Proc. Natl. Acad. Sci. U.S.A.* **97**, 8151–8156 (2000).
13. M. Cui, G. Qin, K. Yu, M. S. Bowers, M. Zhang, Targeting the small- and intermediate-conductance Ca^{2+}-activated potassium channels: The drug-binding pocket at the channel/calmodulin interface. *Neurosignals* **22**, 65–78 (2014).
14. X. M. Xia, B. Fakler, A. Rivard, G. Wayman, T. Johnson-Pais, J. E. Keen, T. Ishii, B. Hirschberg, C. T. Bond, S. Lutsenko, J. Maylie, J. P. Adelman, Mechanism of calcium gating in small-conductance calcium-activated potassium channels. *Nature* **395**, 503–507 (1998).
15. W. Li, D. B. Halling, A. W. Hall, R. W. Aldrich, EF hands at the N-lobe of calmodulin are required for both SK channel gating and stable SK–calmodulin interaction. *J. Gen. Physiol.* **134**, 281–293 (2009).
16. M. A. Schumacher, M. Crum, M. C. Miller, Crystal structures of apocalmodulin and an apocalmodulin/SK potassium channel gating domain complex. *Structure* **12**, 849–860 (2004).
17. M. A. Schumacher, A. F. Rivard, H. P. Bächinger, J. P. Adelman, Structure of the gating domain of a Ca^{2+}-activated K$^+$ channel complexed with Ca^{2+}/calmodulin. *Nature* **410**, 1120–1124 (2001).
18. M. Zhang, C. Abrams, L. Wang, A. Gizzi, L. He, R. Lin, Y. Chen, P. J. Loll, J. M. Pascal, J. F. Zhang, Structural basis for calmodulin as a dynamic calcium sensor. *Structure* **20**, 911–923 (2012).
19. M. Zhang, J. M. Pascal, J. F. Zhang, Unstructured to structured transition of an intrinsically disordered protein peptide in coupling Ca^{2+}-sensing and SK channel activation. *Proc. Natl. Acad. Sci. U.S.A.* **110**, 4828–4833 (2013).
20. D. E. Logothetis, V. I. Petrou, S. K. Adney, R. Mahajan, Channelopathies linked to plasma membrane phosphoinositides. *Pflugers Arch.* **460**, 321–341 (2010).
21. B. C. Suh, B. Hille, PIP$_2$ is a necessary cofactor for ion channel function: How and why? *Annu. Rev. Biophys.* **37**, 175–195 (2008).
22. D. E. Logothetis, V. I. Petrou, M. Zhang, R. Mahajan, X. Y. Meng, S. K. Adney, L. Cui, L. Baki, Phosphoinositide control of membrane protein function: A frontier led by studies on ion channels. *Annu. Rev. Physiol.* **77**, 81–104 (2015).
23. C. M. Lopes, H. Zhang, T. Rohacs, T. Jin, J. Yang, D. E. Logothetis, Alterations in conserved Kir channel-PIP$_2$ interactions underlie channelopathies. *Neuron* **34**, 933–944 (2002).
24. T. Rohács, C. M. Lopes, T. Jin, P. P. Ramdya, Z. Molnár, D. E. Logothetis, Specificity of activation by phosphoinositides determines lipid regulation of Kir channels. *Proc. Natl. Acad. Sci. U.S.A.* **100**, 745–750 (2003).
25. S. B. Hansen, X. Tao, R. MacKinnon, Structural basis of PIP$_2$ activation of the classical inward rectifier K$^+$ channel Kir2.2. *Nature* **477**, 495–498 (2011).
26. M. R. Whorton, R. MacKinnon, Crystal structure of the mammalian GIRK2 K$^+$ channel and gating regulation by G proteins, PIP$_2$, and sodium. *Cell* **147**, 199–208 (2011).
27. M. Zhang, X. Y. Meng, M. Cui, J. M. Pascal, D. E. Logothetis, J. F. Zhang, Selective phosphorylation modulates the PIP$_2$ sensitivity of the CaM–SK channel complex. *Nat. Chem. Biol.* **10**, 753–759 (2014).
28. M. Zhang, J. M. Pascal, M. Schumann, R. S. Armen, J. F. Zhang, Identification of the functional binding pocket for compounds targeting small-conductance Ca^{2+}-activated potassium channels. *Nat. Commun.* **3**, 1021 (2012).
29. H. Zhang, L. C. Craciun, T. Mirshahi, C. M. Lopes, T. Jin, D. E. Logothetis, PIP$_2$ activates KCNQ channels, and its hydrolysis underlies receptor-mediated inhibition of M currents. *Neuron* **37**, 963–975 (2003).
30. X. Du, H. Zhang, C. Lopes, T. Mirshahi, T. Rohacs, D. E. Logothetis, Characteristic interactions with phosphatidylinositol 4,5-bisphosphate determine regulation of Kir channels by diverse modulators. *J. Biol. Chem.* **279**, 37271–37281 (2004).
31. D. Allen, B. Fakler, J. Maylie, J. P. Adelman, Organization and regulation of small conductance Ca^{2+}-activated K$^+$ channel multiprotein complexes. *J. Neurosci.* **27**, 2369–2376 (2007).
32. W. Bildl, T. Strassmaier, H. Thurm, J. Andersen, S. Eble, D. Oliver, M. Knipper, M. Mann, U. Schulte, J. P. Adelman, B. Fakler, Protein kinase CK2 is coassembled with small conductance Ca^{2+}-activated K$^+$ channels and regulates channel gating. *Neuron* **43**, 847–858 (2004).
33. F. Maingret, B. Coste, J. Hao, A. Giamarchi, D. Allen, M. Crest, D. W. Litchfield, J. P. Adelman, P. Delmas, Neurotransmitter modulation of small-conductance Ca^{2+}-activated K$^+$ channels by regulation of Ca^{2+} gating. *Neuron* **59**, 439–449 (2008).
34. K. A. Buchanan, M. M. Petrovic, S. E. Chamberlain, N. V. Marrion, J. R. Mellor, Facilitation of long-term potentiation by muscarinic M$_1$ receptors is mediated by inhibition of SK channels. *Neuron* **68**, 948–963 (2010).
35. A. J. Giessel, B. L. Sabatini, M1 muscarinic receptors boost synaptic potentials and calcium influx in dendritic spines by inhibiting postsynaptic SK channels. *Neuron* **68**, 936–947 (2010).
36. J. Wang, D. A. Richards, Segregation of PIP2 and PIP3 into distinct nanoscale regions within the plasma membrane. *Biol. Open* **1**, 857–862 (2012).
37. I. E. Michailidis, R. Rusinova, A. Georgakopoulos, Y. Chen, R. Iyengar, N. K. Robakis, D. E. Logothetis, L. Baki, Phosphatidylinositol-4,5-bisphosphate regulates epidermal growth factor receptor activation. *Pflugers Arch.* **461**, 387–397 (2011).
38. P. J. Hamilton, A. N. Belovich, G. Khelashvili, C. Saunders, K. Erreger, J. A. Javitch, H. H. Sitte, H. Weinstein, H. J. Matthies, A. Galli, PIP$_2$ regulates psychostimulant behaviors through its interaction with a membrane protein. *Nat. Chem. Biol.* **10**, 582–589 (2014).
39. G. M. Morris, D. S. Goodsell, R. S. Halliday, R. Huey, W. E. Hart, R. K. Belew, A. J. Olson, Automated docking using a Lamarckian genetic algorithm and an empirical binding free energy function. *J. Comput. Chem.* **19**, 1639–1662 (1998).
40. C. M. Breneman, K. B. Wiberg, Determining atom-centered monopoles from molecular electrostatic potentials. The need for high sampling density in formamide conformational analysis. *J. Comp. Chem.* **11**, 361–373 (1990).

41. M. J. Frisch, G. W. Trucks, H. B. Schlegel, G. E. Scuseria, M. A. Robb, J. R. Cheeseman, V. G. Zakrzewski, J. A. Montgomery, Gaussian 98 (Gaussian Inc., Pittsburgh, PA, 2001).

42. X. Y. Meng, H. X. Zhang, D. E. Logothetis, M. Cui, The molecular mechanism by which PIP$_2$ opens the intracellular G-loop gate of a Kir3.1 channel. *Biophys. J.* **102**, 2049–2059 (2012).

43. K. J. Bowers, E. Chow, H. Xu, R. O. Dror, M. P. Eastwood, B. A. Gregersen, J. L. Klepeis, I. Kolossvary, M. A. Moraes, F. D. Sacerdoti, J. K. Salmon, Y. Shan, D. E. Shaw, in *Proceedings of the ACM/IEEE Conference on Supercomputing (SC06)* (IEEE, New York, 2006), pp. 11–17.

Science Advances

Molecular overlap in the regulation of SK channels by small molecules and phosphoinositides

Miao Zhang, Xuan-Yu Meng, Ji-fang Zhang, Meng Cui and Diomedes E. Logothetis

ARTICLE TOOLS	http://advances.sciencemag.org/content/1/6/e1500008
SUPPLEMENTARY MATERIALS	http://advances.sciencemag.org/content/suppl/2015/07/07/1.6.e1500008.DC1
REFERENCES	This article cites 40 articles, 7 of which you can access for free http://advances.sciencemag.org/content/1/6/e1500008#BIBL
PERMISSIONS	http://www.sciencemag.org/help/reprints-and-permissions